MgO:PPLN 中红外光参量振荡器的闲频光纵模特性研究

郑 浩[1,2], 赵 臣[3], 张 飞[1,2], 李鹏飞[1,2], 颜秉政[1,2], 王雨雷[1,2], 白振旭[1,2*], 吕志伟[1,2*]

(1. 河北工业大学 先进激光技术研究中心，天津 300401;
2. 河北省先进激光技术与装备重点实验室，天津 300401;
3. 电磁空间安全全国重点实验室，天津 300308)

摘 要：文中介绍了一种纳秒脉冲端面泵浦 MgO:PPLN 外腔光参量振荡器。基频光采用激光二极管泵浦的声光调 Q Nd:YVO_4 纳秒激光器，在声光 Q 开关的工作重复频率为 120 kHz 时，实现脉宽 8.1 ns、最高输出功率 7.03 W 的 1.064 μm 激光输出。通过将基频光聚焦至 MgO:PPLN 晶体内，外腔泵浦得到了脉冲宽度为 4.7 ns，输出功率 0.7 W 的 3 μm 闲频光。基频光-闲频光转换效率为 9.95%，将基频光与闲频光的时域波形图傅里叶变换后对比，观察到光参量振荡过程对闲频光高阶纵模的抑制现象。该研究对实现窄线宽低噪声的中红外激光具有一定的参考价值。

关键词：光参量振荡器； MgO:PPLN； 纵模； 中红外； 闲频光

中图分类号：TN248 **文献标志码：**A **DOI：**10.3788/IRLA20230378

0 引 言

窄线宽全固态激光器以其高相干性、低噪声和高光束质量等优点，在高精度精密测量、相干通信、光学传感、量子光学等领域有着重要应用[1−3]。而具有特定波长的窄线宽激光器是满足特定离子、分子和材料等吸收或透过的前提，因此开展不同波长和运转方式激光的纵模特性研究具有重要的实际意义[4−6]。3~5 μm 中红外激光位于大气窗口，在大气中对浓雾、烟尘和灰尘有着较强的穿透性，且在海平面上的传播被气体分子吸收程度小[7−9]。同时，3~5 μm 波段涵盖了大部分分子的光谱谱线，例如甲烷、乙烷、硫化氢、水蒸气等气体，因此被称为分子的“指纹谱”，是实现特殊气体监测的优质光源[10−14]。目前，3~5 μm 中红外激光器已在环境气体监测、光谱分析、光电对抗等方面有着重要应用。

目前，利用激光增益介质直接产生 3~5 μm 中红外激光辐射的技术路线尚不成熟，因此人们往往通过非线性频率变换的方式将常规波段激光变换至 3~5 μm。MgO:PPLN 晶体具有高的二阶非线性系数、较高的抗损伤阈值和可实现波长调谐输出等优势，被广泛应用于光参量振荡器 (OPO) 中获得 3~5 μm 中红外激光[15−18]。

由相关报道可知，非线性光学转换过程在实现频率变换的同时也能够实现单纵模和噪声抑制[19−21]。早在 1997 年，英国南安普顿大学的 Martin 等人利用激光振荡器内二次谐波引入的损耗和色散效应，有效抑制了纵模模式跳变，实现了大范围调谐的单频激光输出[22]。2016 年，澳大利亚麦考瑞大学 Mildren 团队利用受激散射增益介质的无空间烧孔特性，在不增加额外的模式选择元件的情况下，通过 1 μm 波段泵浦光实现了 1.2 μm 的外腔拉曼振荡器的单纵模运转[23]。2019 年，该团队在腔内插入二次谐波产生元件，实现了 0.6 μm 可见光波段的金刚石拉曼激光的单纵模运转[24]。2023 年，国科大杭州高等研究院 Li 等人在 V 型腔结构的金刚石拉曼振荡器中插入二次谐波晶体，实现了受激布里渊散射和级联拉曼散射的抑制，获得了拉曼激光的单纵模运转[25]。上述报道中可

收稿日期:2023−06−20； **修订日期:**2023−08−21

基金项目:国家自然科学基金项目 (61927815, 62075056); 天津市自然科学基金项目 (22JCYBJC01100)

作者简介:郑浩，男，博士生，主要从高功率固体激光技术方面的研究。

导师(通讯作者)简介:吕志伟，男，教授，博士，主要从事高功率激光技术与非线性光学方面的研究。

通讯作者:白振旭，男，教授，博士生导师，博士，主要从事高功率激光技术与新型激光器方面的研究。

见，通过二次谐波以及三阶非线性光学效应已经实现了振荡器内纵模的有效抑制。但是针对 OPO 闲频光纵模的相关研究却鲜有报道。

文中以 MgO:PPLN 作为非线性光学频率变换晶体开展其中红外 OPO 中纵模特性的研究。理论模拟了 MgO:PPLN-OPO 输出波长随温度的调谐曲线，实验上通过声光调 Q 的 Nd:YVO_4 激光器输出的多纵模 1 064 nm 基频光泵浦 MgO:PPLN-OPO，实现了少纵模和噪声抑制的 3 μm 闲频光输出。该研究对 OPO 中的纵模特性调控以及实现低噪声的参量光输出具有一定的参考价值。

1 实验原理及装置

首先，基于相位匹配公式 (1) 与色散方程 (2)，对固定周期 MgO:PPLN 晶体的温度调谐曲线进行计算，得到[26−27]：

$$\frac{n_p}{\lambda_p}-\frac{n_s}{\lambda_s}-\frac{n_i}{\lambda_i}-\frac{1}{\Lambda}=0 \tag{1}$$

$$n_e^2=a_1+b_1f(T)+\frac{a_2+b_2f(T)}{\lambda^2-(a_3+b_3f)^2}+\frac{a_4+b_4f(T)}{\lambda^2-a_5^2}-a_6\lambda^2 \tag{2}$$

式中：Λ 为晶体极化周期；$f(T)$ 为以温度为自变量的函数；a_i、b_i 为常数；$n_j(j=i、s、p$ 分别为信号光、闲频光、泵浦光) 为折射率；$\lambda_j(j=i、s、p$ 分别为信号光、闲频光、泵浦光) 为激光波长。晶体极化周期 Λ=31 μm (与后续实验采用的相一致)，输出波长随温度的调谐曲线如图 1 所示，当环境温度为 20 ℃ 时，闲频光的理论输出波长为 3.226 μm。

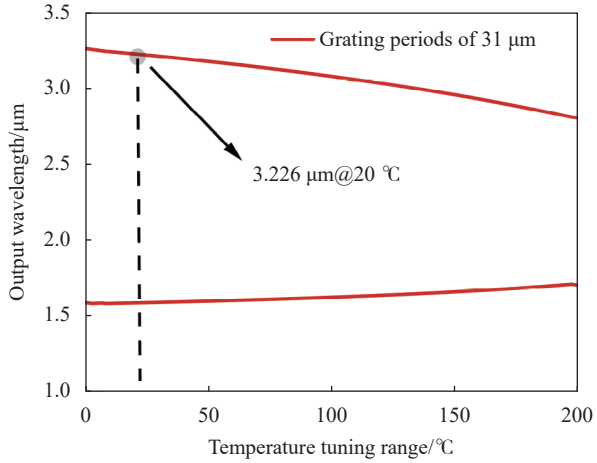

图 1 温度调谐曲线

Fig.1 Temperature tuning curve

实验装置如图 2 所示，泵浦源为 808 nm 的激光二极管连续激光器，通过纤芯直径 400 μm，数值孔径 0.22 的光纤耦合输出。使用 1∶2 的光纤输出聚焦镜将泵浦光聚焦到 Nd:YVO_4 晶体中，焦点处泵浦光光斑半径为 400 μm，实验中使用 a 切 Nd:YVO_4 晶体，尺寸为 3 mm×3 mm×18 mm，掺杂浓度为 0.3%。平面镜 M1 与 M2 组成 1 064 nm 基频光谐振腔，利用声光 Q 开关 (Gooch & Housego 公司，I-QS080-1.5C10G-4-HR6) 对基频光调制，腔长总长为 95 mm。基频光输出后通过 50 mm 的聚焦镜 f，将 1 064 nm 的基频光汇聚到 MgO:PPLN 晶体中，基频光在焦点处的光斑半径为 400 μm，MgO:PPLN 晶体尺寸为 10.5 mm×1 mm×20 mm，晶体掺杂浓度 5%，极化周期为 31.0 μm。平面镜 M3 与 M4 组成的参量光谐振腔，谐振腔长度为 56 mm，最终由 M4 输出 3 μm 闲频光。实验装置中镜片的参数如表 1 所示。

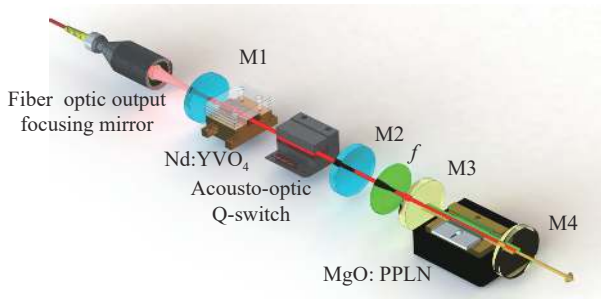

图 2 实验装置示意图

Fig.2 Diagram of experimental setup

表 1 实验装置中镜片参数

Tab.1 Lens parameters in experimental setup

Elements	Parameters
M1	AR@808 nm&HR@1 064 nm plane
M2	HT@1 064 nm T=20% plane
M3	S1:AR@1 064 nm&HR@3 200-4 200 nm & HR@1 400-2 000 nm S2:AR@1 064 nm plane
M4	S1:HR@1 064 nm&HT@3 200-4 200 nm & HR@1 400-2 000 nm S2:AR@3 200-4 200 nm plane
f	AR@1 064 nm f=50 mm

2 实验结果与分析

1 064 nm 基频光的输出功率随泵浦光功率的变化，如图 3 所示。基频光连续最高输出功率 9.1 W。

在基频光腔内加入声光 Q 开关后，腔内衍射损耗增大，造成脉冲基频光的功率相较连续光有所降低，当重复频率为 120 kHz 时获得的最高输出功率降低至 7.03 W。但无论是连续光还是脉冲光，输出功率并没有明显抖动或者下降趋势，未来有望通过增加泵浦光功率实现进一步提高。

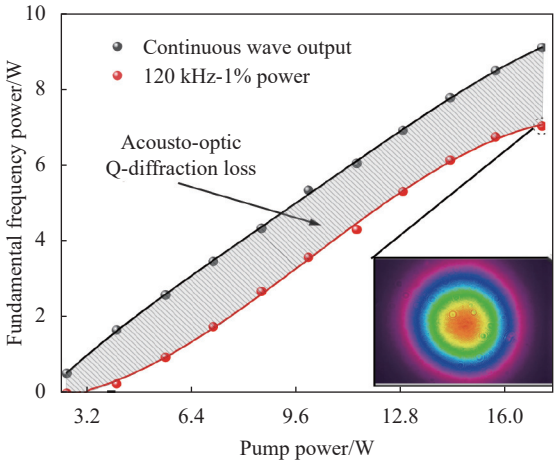

图 3 1064 nm 基频光输出功率曲线 (插图: 最高功率输出调 Q 激光的光束空间分布)

Fig.3 Output power curve of 1064 nm fundamental frequency (inset: beam profile of the Q-switched output at maximum pump power)

将基频光耦合到 MgO:PPLN 晶体中，进行光参量振荡，输出闲频光功率随基频光功率变化如图 4 所示，在室温 20 ℃，基频光功率为 7.03 W 时，获得了波长为 3.196 μm (见插图)，输出功率为 0.702 W 的闲频光，这与之前的理论预测基本一致。由于腔镜设有对信号光反射率高于 90% 的高反膜，因此输出的信号光较弱，测量精度要求高难度较大，并且信号光不作为文中研究重点，故不对其过多叙述。

测得的基频光与闲频光的时域波形图如图 5(a) 所示。基频光脉冲宽度为 8.1 ns，可以看出基频光中存在多纵模，并伴随着一定程度的噪声。对应输出的 3 μm 闲频光的脉冲宽度为 4.7 ns，相较于基频光脉冲宽度有所压窄，且波形更加平滑，这意味着相对于基频光的纵模有所抑制。为了更清晰地观察纵模和噪声的变化，将基频光和闲频光的脉冲波形图进行一次傅里叶变换，得到结果如图 5(b) 所示。从图中可以看出，基频光为多纵模输出且存在较为明显的噪声，而经过光参量振荡过程后，闲频光的

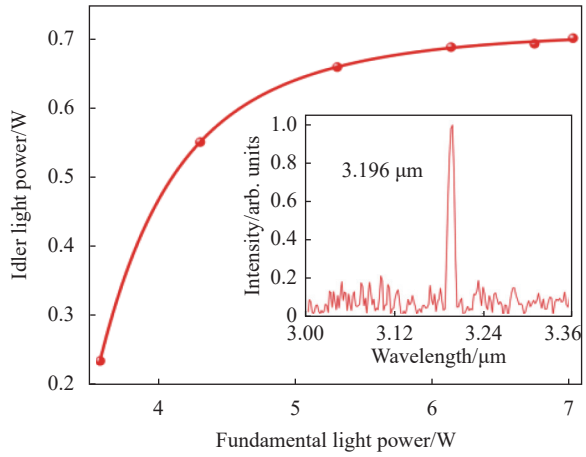

图 4 3 μm 闲频光输出功率 (插图: 光谱图)

Fig.4 Output power of 3 μm idler light (inset: spectrum)

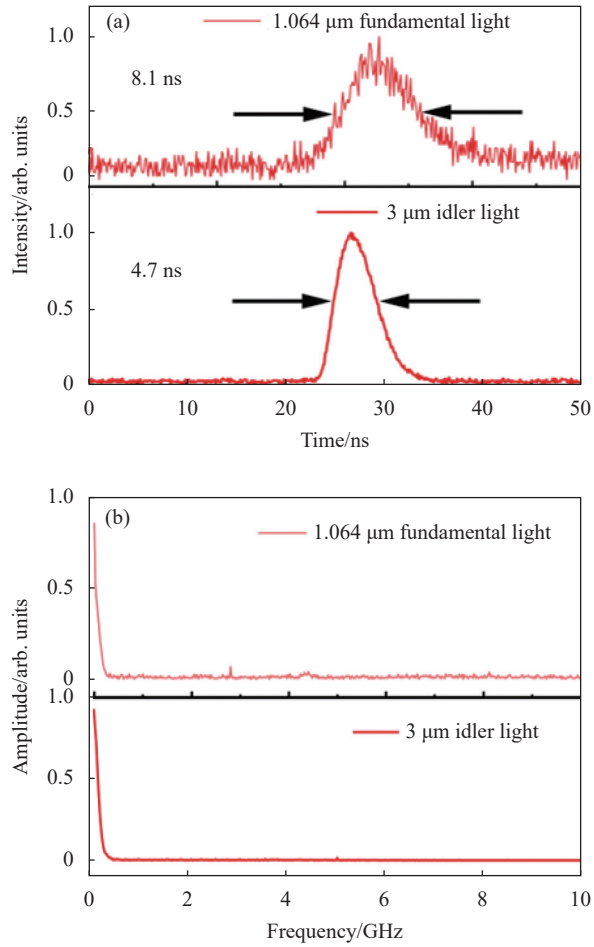

图 5 基频光和闲频光的输出特性对比。(a) 时域; (b) 傅里叶变换域

Fig.5 Comparison of output characteristics of fundamental frequency and idle light. (a) Time-domain; (b) Fourier transform domain

纵模被明显的抑制了，这与时域观察到的结果相一致。

3 结 论

通过 808 nm 的激光二极管泵浦 Nd:YVO_4 晶体实现了重复频率 120 kHz, 脉宽 8.1 ns, 最高 7.03 W 的多纵模基频光输出, 泵浦光-基频光转换效率为 40.9%。进行 OPO 实验得到了脉冲宽度为 4.7 ns, 输出功率 0.7 W 的 3 μm 闲频光, 基频光-闲频光转换效率 9.95%, 将基频光与闲频光的时域波形图进行傅里叶变换后对比, 可以观察到光参量振荡过程对闲频光纵模的抑制现象。该现象为 OPO 的纵模抑制技术提供了实验参考。

参考文献:

[1] Bai Zhenxu, Zhao Zhongan, Tian Menghan, et al. A comprehensive review on the development and applications of narrow-linewidth lasers [J]. ***Microwave and Optical Technology Letters***, 2022, 64(12): 2244-2255.

[2] Peng Weina, Jin Pixian, Li Fengqin, et al. A review of the high-power all-solid-state single-frequency continuous-wave laser [J]. ***Micromachines***, 2021, 12(11): 1426.

[3] Shi Wei, Fu Shijie, Sheng Quan, et al. Research progress on high-performance single-frequency fiber lasers: 2017-2021 (*invited*) [J]. ***Infrared and Laser Engineering***, 2022, 51(1): 20210905. (in Chinese)

[4] Fu Shijie, Shi Wei, Feng Yan, et al. Review of recent progress on single-frequency fiber lasers [J]. ***JOSA B***, 2017, 34(3): A49-A62.

[5] Granados E, Stoikos G. Spectral purification of single-frequency Stokes pulses in doubly resonant integrated diamond resonators [J]. ***Optics Letters***, 2022, 47(16): 3976-3979.

[6] Huo X, Qi Y, Zhang Y, et al. Research development of 589 nm laser for sodium laser guide stars [J]. ***Optics and Lasers in Engineering***, 2020, 134: 106207.

[7] Yu Y, Chen X, Cheng L, et al. Continuous-wave 1.57 μm/3.84 μm intra-cavity multiple optical parametric oscillator based on MgO: APLN [J]. ***Acta Physica Sinica***, 2015, 64(22): 224215. (in Chinese)

[8] Yue Wei, Han Yongchang, Dongye S, et al. Development of large-sized silicon substrate 633 nm and 3.5-4.1 μm dual-band high reflection coatings [J]. ***Infrared and Laser Engineering***, 2012, 41(7): 1854-1857. (in Chinese)

[9] Bai Z, Zhao C, Gao J, et al. Optical parametric oscillator with adjustable pulse width based on $KTiOAsO_4$ [J]. ***Optical Materials***, 2023, 136: 13506.

[10] Wang Yuheng, Liu Heyan, Wang Zeyu, et al. 4.1 μm high power mid-infrared intracavity optical parametric oscillator [J]. ***Acta Photonica Sinica***, 2019, 48(8): 0823002. (in Chinese)

[11] Huang Jiayu, Lin Haifeng, Yan Peiguang. Highly efficient, widely tunable fan-out MgO:PPLN mid-infrared optical parametric oscillator [J]. ***Infrared and Laser Engineering***, 2023, 52(5): 20220605. (in Chinese)

[12] Abulikemu Aiziheerjiang, Jiashaner Dana, Yuxia Zhou, et al. High-beam-quality idler-resonant mid-infrared optical parametric oscillator based on MgO:PPLN [J]. ***Infrared and Laser Engineering***, 2023, 52(4): 0214001. (in Chinese)

[13] Wang Feifei, Li Jiatong, Sun Xiaohui, et al. High-power and high-efficiency 4.3 μm ZGP-OPO [J]. ***Chinese Optics Letters***, 2022, 20(1): 79-83.

[14] Jiang Xingchen, Cheng Dehua, Li Yeqiu, et al. Research on mid-infrared laser at 35 kHz based on optical parametric oscillator [J]. ***Infrared and Laser Engineering***, 2022, 51(9): 20210817. (in Chinese)

[15] Ge Jinzhu, Wang Zijian, Wang Yuheng, et al. Study on high efficiency 3.4 μm optical parametric oscillation based on external cavity MgO:PPLN pumped by fiber laser [J]. ***Journal of Changchun University of Science and Technology (Natural Science Edition)***, 2023, 46(1): 1-6.

[16] Chen Bingyan, Yu Yongji, Wu Chunting, et al. High efficiency mid-infrared 3.8 μm MgO: PPLN optical parametric oscillator pumped by narrow linewidth 1064 nm fiber laser [J]. ***Chinese Optics***, 2021, 14(2): 361-367.

[17] Zhao Zhigang, Liu Hu, Wang Defei, et al. 3.705 μm compact optical parametric oscillator [J]. ***Laser & Infrared***, 2019, 49(1): 51-54. (in Chinese)

[18] Niu Yaru, Yan Xing, Chen Jiaxuan, et al. Research progress on periodically poled lithium niobate for nonlinear frequency conversion [J]. ***Infrared Physics & Technology***, 2022, 125: 104243.

[19] Zhang Kuanshou, Lu Huadong, Li Yuanji, et al. Progress on high-power low-noise continuous-wave single-frequency all-solid-state lasers [J]. ***Chinese Journal of Lasers***, 2021, 48(5): 0501002. (in Chinese)

[20] Li Muye, Yang Xuezong, Sun Yuxiang, et al. Single-frequency continuous-wave diamond Raman laser (Invited) [J]. ***Infrared and Laser Engineering***, 2022, 51(6): 20210970. (in Chinese)

[21] Jin D, Bai Z, Lu Z, et al. 22.5 W narrow-linewidth diamond Brillouin laser at 1064 nm [J]. ***Optics Letters***, 2022, 47(20): 5360-5363.

[22] Martin K I, Clarkson W A, Hanna D C. Self-suppression of axial

mode hopping by intracavity second-harmonic generation [J]. *Optics Letters*, 1997, 22(6): 375-377.

[23] Lux O, Sarang S, Kitzler O, et al. Intrinsically stable high-power single longitudinal mode laser using spatial hole burning free gain [J]. *Optica*, 2016, 3(8): 876-881.

[24] Yang X, Kitzler O, Spence D J, et al. Single-frequency 620 nm diamond laser at high power, stabilized via harmonic self-suppression and spatial-hole-burning-free gain [J]. *Optics Letters*, 2019, 44(4): 839-842.

[25] Li Muye, Yang Xuezong, Sun Yuxiang, et al. Single-longitudinal mode operation and stimulated Brillouin scattering suppression in a diamond Raman laser [J]. *Optics Express*, 2023, 31(5): 8622-8631.

[26] Wang Yuheng. Study on Nd: MgO:PPLN in infrared self-optical parametric oscillator[D]. Changchun: Changchun University of Science and Technology, 2019. (in Chinese)

[27] Wang Zijian. Study on 1 064 nm master oscillator power amplifier pumped PPMgLN mid-infrared optical parametric oscillator [D]. Changchun: Changchun University of Science and Technology, 2016. (in Chinese)

Study on the longitudinal mode characteristic of idler wave in MgO:PPLN infrared optical parametric oscillator

Zheng Hao[1,2], Zhao Chen[3], Zhang Fei[1,2], Li Pengfei[1,2], Yan Bingzheng[1,2], Wang Yulei[1,2], Bai Zhenxu[1,2*], Lv Zhiwei[1,2*]

(1. Center for Advanced Laser Technology, Hebei University of Technology, Tianjin 300401, China;
2. Hebei Key Laboratory of Advanced Laser Technology and Equipment, Tianjin 300401, China;
3. National Key Laboratory of Electromagnetic Space Security, Tianjin 300308, China)

Abstract:

Objective Narrow linewidth solid-state lasers are characterized by their excellent coherence and beam quality. Narrow linewidth lasers of certain wavelengths are necessary to meet the absorption or transmission requirements of specific ions, molecules, and materials. Therefore, it is of great significant to investigate the longitudinal mode characteristics of lasers at different wavelengths and operating modes. The 3-5 μm spectral range falls within the atmospheric window. Mid-infrared lasers in this band have been widely used for environmental gas monitoring, spectral analysis and optoelectronic countermeasures. Currently, MgO:PPLN crystals are typically employed in optical parametric oscillators (OPOs) to generate mid-infrared lasers within the 3-5 μm spectrum. This is attributed to their high second-order nonlinearity coefficient, large damage threshold, and widely tunable wavelength range. In addition to the tunability of the output wavelength, the optical parametric oscillation process also possesses the ability to suppress multi-longitudinal-mode operation within the cavity. While previous experiments have demonstrated that multi-longitudinal-mode operation can be suppressed by placing optical parametric crystals inside the cavity, However, more specific studies are limited. In this study, a comparative analysis of the variation of longitudinal mode properties at fundamental and idler frequencies was performed using MgO:PPLN crystals.

Methods The output wavelength at different temperatures is simulated based on the phase matching equation and the dispersion equation, as depicted in Fig.1. The experimental setup is illustrated in Fig.2. An fiber coupled 808 nm laser diode continuous-wave laser was used as the pump source, with a core diameter of 200 μm and numerical aperture of 0.22. A 1:2 focusing lens result in a spot radius of 400 μm at the Nd:YVO_4 crystal. The crystal has a dimension of 3 mm×3 mm×18 mm and a doping concentration of 0.3%. Plane mirrors M1 and M2 form a 1 064 nm fundamental frequency optical resonator with a cavity length of 95 mm. A Q-switched pulse output of the fundamental frequency was obtained using an acousto-optic modulator. The fundamental frequency wave was

directly coupled into the MgO:PPLN crystal via a 50 mm focusing lens, resulting in a beam radius of 400 μm for the fundamental frequency wave. The MgO:PPLN crystal, with dimensions of 10.5 mm ×1 mm×20 mm, a doping concentration of 5%, and a poling period of 31.0 μm was used. The OPO consist of plane mirrors M3 and M4 with a cavity length of 56 mm. The coating parameters of the lenses used in the experiments are presented in Tab.1.

Results and Discussions Figure 3 depicts the output power variation of the 1 064 nm fundamental frequency wave with the pump wave. A Q-switched laser output with a maximum power of 7.03 W is obtained at a repetition frequency of 120 kHz. Figure 4 illustrates the variation of output idle frequency optical power with the fundamental frequency. At a room temperature of 20 ℃ and a fundamental frequency optical power of 7.03 W, an idle frequency light with an output power of 0.702 W and a wavelength of 3.196 μm is obtained, corresponding to a conversion efficiency of 9.95%. Figure 5(a) shows the time-domain waveforms of the measured fundamental and idle frequencies. The pulse width of the 3 μm idle frequency laser is 4.7 ns, which is slightly narrower compared to the fundamental frequency laser and has a smoother waveform. Fourier transforms are performed on the waveforms, as shown in Fig.5(b). It can be seen that the multiple longitudinal modes are significantly suppressed after the OPO process, consistent with the results observed in the time domain.

Conclusions By pumping the Nd:YVO_4 crystal with an 808 nm laser diode, multiple longitudinal mode output of the fundamental frequency wave with a repetition rate of 120 kHz and a pulse width of 8.1 ns was achieved, resulting in a maximum output power of 7.03 W. Based on this fundamental frequency pump source, an MgO:PPLN-OPO was developed, yielding a pulse width of 4.7 ns and an output power of 0.7 W for the 3 μm idler wave, with a fundamental-to-idler wave conversion efficiency of 9.95%. Comparing the Fourier-transformed temporal waveforms of the fundamental frequency and idler waves, we can clearly observe the suppression of higher-order longitudinal modes of the idler wave during the OPO process. This study has significant reference value for regulating the longitudinal mode characteristics in OPO and achieving low noise parametric optical output.

Key words: optical parametric oscillator; MgO:PPLN; longitudinal-mode; mid-infrared; idler

Funding projects: National Natural Science Foundation of China (61927815, 62075056)；Natural Science Foundation of Tianjin (22JCYBJC01100)